Designing iron-doped basic magnesium sulfate photocatalyst for wide spectral photoresponse and superior catalytic activity

Zhongmei Song [†,‖], Huifang Zhang [†,*], Liang Ma[†,‖], Qinghong Li [†,‖], Siyuan Zhang [†], Chunyan Wang [†], Chengyou Wu[‡,*], Xuefeng Yu [§], Zhen Ma [§], Haining Liu [†,*], Xiushen Ye [†], Zhijian Wu[†]

[†] *Key Laboratory of Green and High-end Utilization of Salt Lake Resources, Qinghai Institute of Salt Lakes, Chinese Academy of Sciences, Xining 810008, China*

[‡] *Qinghai University, Xining 810016, China*

[§] *Qinghai Salt Lake Industry Co., Ltd., Golmud 816000, China*

[‖] *University of Chinese Academy of Sciences, Beijing 100049, China*

Contents:

[*] Corresponding authors. *E-mail addresses*: zhanghf@isl.ac.cn (H.F. Zhang); wuchengyou86@163.com; liuhn@isl.ac.cn (H.N. Liu).

S1. Photometric determination of organic pollutants

(1) Methyl orange

In the wavelength range of 450~550 nm, the acid methyl orange produced by decomposition exhibits a unique absorption peak. We take 5 mL of the sample solution, add 5 mL of deionized water and 15 mL of phosphate-dihydrogen sodium phosphate (pH=2) buffer solution, and mix thoroughly. The absorbance is measured at 505 nm. Quantitative measurement of methyl orange concentration can be done using a linear relationship between absorbance and methyl orange concentration (Figure S1a).

(2) Phenol

Phenolic compounds react with 4-aminoantipyrine in the presence of potassium ferricyanide at pH=10 to produce a reddish-brown product, whose absorbance at 510 nm is linearly related to the concentration of phenolic substances in the liquid phase. Take an appropriate amount of sample solution, add 0.5 mL of ammonia-ammonium chloride buffer (pH=10), 1 mL of 2 wt% 4-aminoantipyrine solution, and 1 mL of 8 wt% potassium ferricyanide solution, and dilute to 25 mL with deionized water, then measure the absorbance at 510 nm. Quantitative measurement of phenol concentration can be done using a linear relationship between absorbance and phenol concentration (Figure S1b).

(3) Ciprofloxacin

Under acidic conditions, ciprofloxacin exhibits characteristic absorption peaks in the range of 200-400 nm. We take 5 mL of the sample solution, dilute it with deionized water to a total volume of 10 mL, and then add 100 mL of 0.05 $mol \cdot L^{-1}$ solution to measure the absorbance at 255 nm. Quantitative measurement of ciprofloxacin concentration can be done using a linear relationship between absorbance and ciprofloxacin concentration (Figure S1c).

(4) Octadecylamine/4-dodecylmorpholine

Under a weak acidic environment, a 1:1 coordination reaction can occur between octadecylamine/4-dodecylmorpholine and methyl orange. The product is bright yellow and soluble in 1,2-dichloroethane. When octadecylamine/4-dodecylmorpholine remains in the lower organic phase and methyl orange enters the upper aqueous phase, the product will decompose under strong acidic conditions. In the wavelength range of 450~550 nm, the acid methyl orange produced by decomposition exhibits a unique absorption peak. Quantitative measurement of octadecylamine/4-dodecylmorpholine concentration can be done using a linear relationship between absorbance and octadecylamine/4-dodecylmorpholine concentration (Figure S1d and e).

S2. Calculation of apparent quantum yield (AQY)

Wavelength of light λ = 326 nm = 326 × 10^{-9} m

Energy of one photon $E = \frac{hc}{\lambda} = \frac{6.6 \times 10^{-34} \times 3 \times 10^{8}}{326 \times 10^{-9}} = 6.07 \times 10^{-19}\, Joules$

The total energy of light falling per second per unit area is

$E_{Total} = 8.72\, W\, cm^{-2} = 8.72 \times 10^{4} W\, m^{-2} = 87200\, W\, m^{-2}$

Number of Photon = $\frac{E_{Total}}{E} = \frac{87200}{6.07 \times 10^{-19}} = 14365.73 \times 10^{19} = 1.44 \times 10^{23}$

Exposed Area =

$\pi r^2 = 3.14 \times 2.5 \times 10^{-2} \times 2.5 \times 10^{-2} = 1.96 \times 10^{-3}\, m^2$

Total number of Photon falling on the catalyst = $1.44 \times 10^{23} \times 1.96 \times 10^{-3}$

$= 2.82 \times 10^{20}$

Apparent quantum yield (AQY) = $\frac{Number\ of\ degraded\ molecule}{Number\ of\ incident\ photon} \times 100\%$

$$(AQY)_{Fe\text{-}BMS\text{-}0.05} = \frac{3.36 \times 10^{19} \times 0.545}{2.82 \times 10^{20}} \times 100\ \% = 6.49\%$$

$$(AQY)_{BMS} = \frac{3.36 \times 10^{19} \times 0.216}{2.82 \times 10^{20}} \times 100\ \% = 2.57\%$$

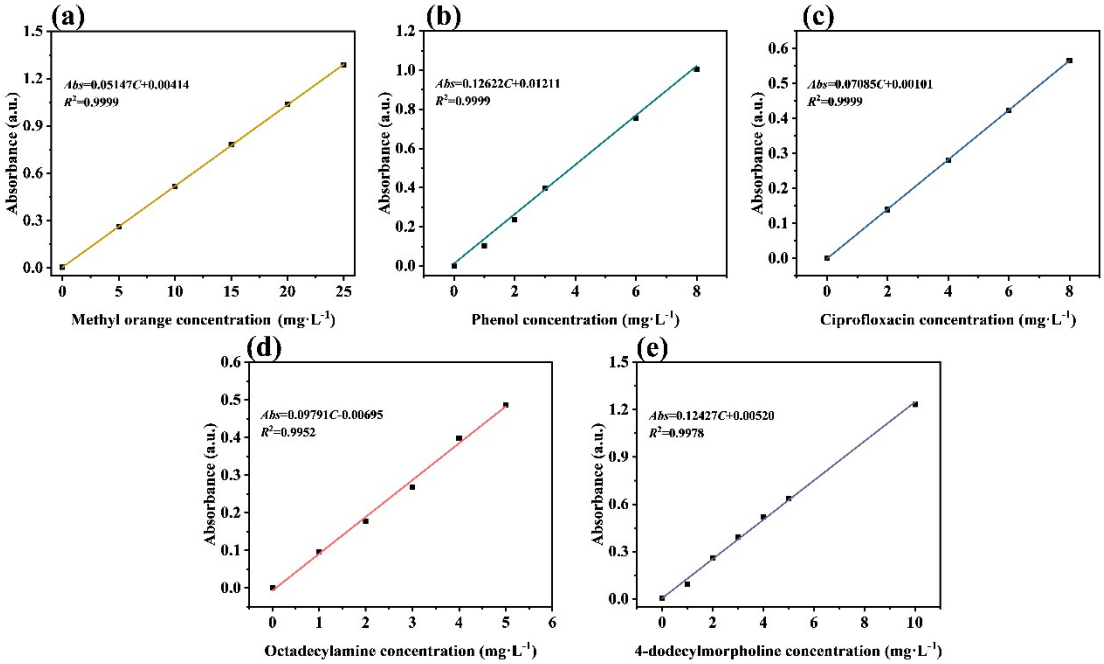

Figure S1. Standard curve of (a) methyl orange, (b) phenol, (c) ciprofloxacin, (d) octadecylamine, (e) 4-dodecylmorpholine.

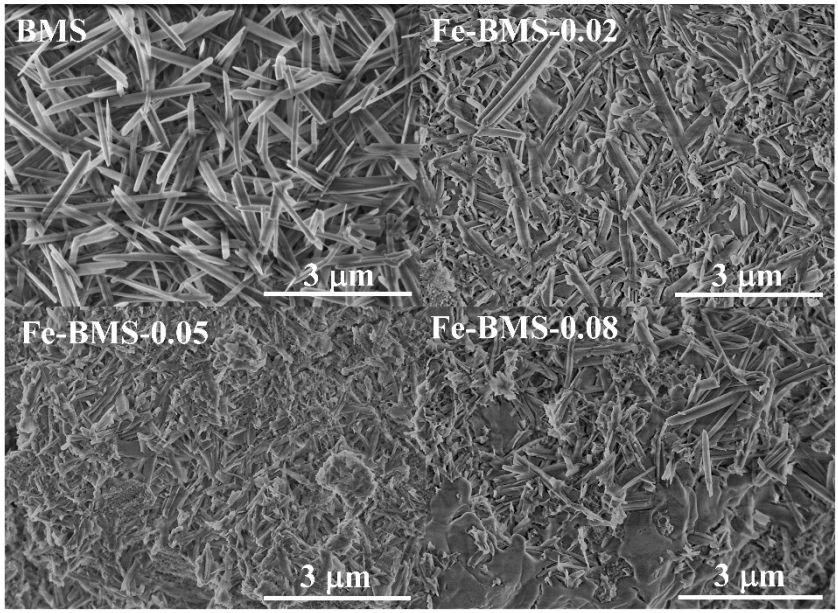

Figure S2 SEM images of BMS and Fe-BMS-x (x= 0.02, 0.05, 0.08)

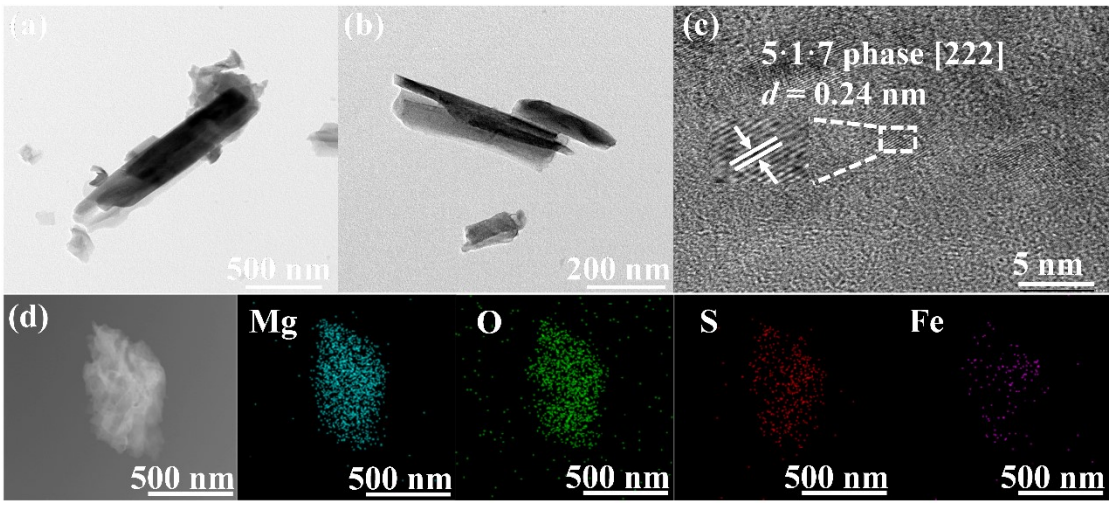

Figure S3. (a, b) TEM images of Fe-BMS-0.02, (c) HRTEM images of Fe-BMS-0.02, (d) HAADF-STEM and corresponding elemental mapping images of Mg, O, S and Fe.

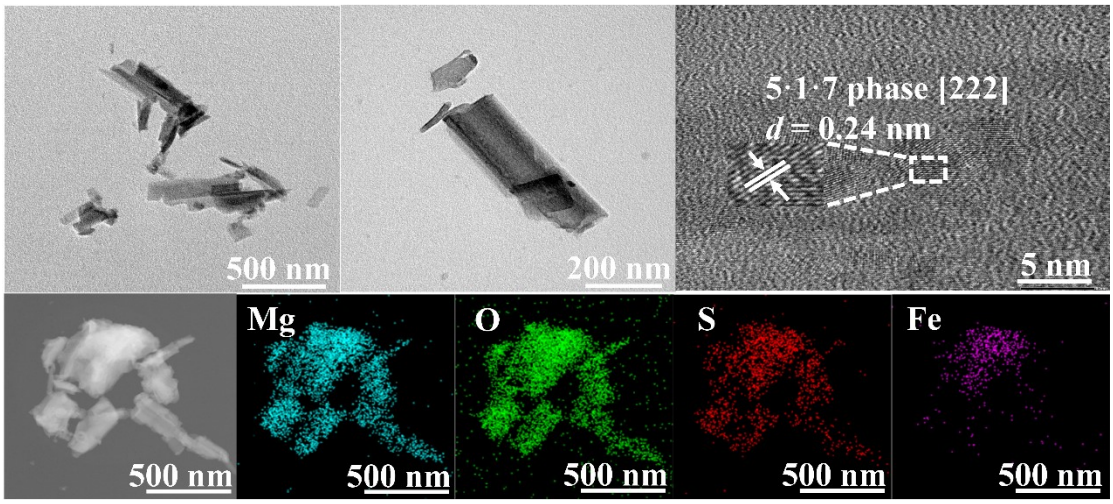

Figure S4. (a, b) TEM images of Fe-BMS-0.05, (c) HRTEM images of Fe-BMS-0.05, (d) HAADF-STEM and corresponding elemental mapping images of Mg, O, S and Fe.

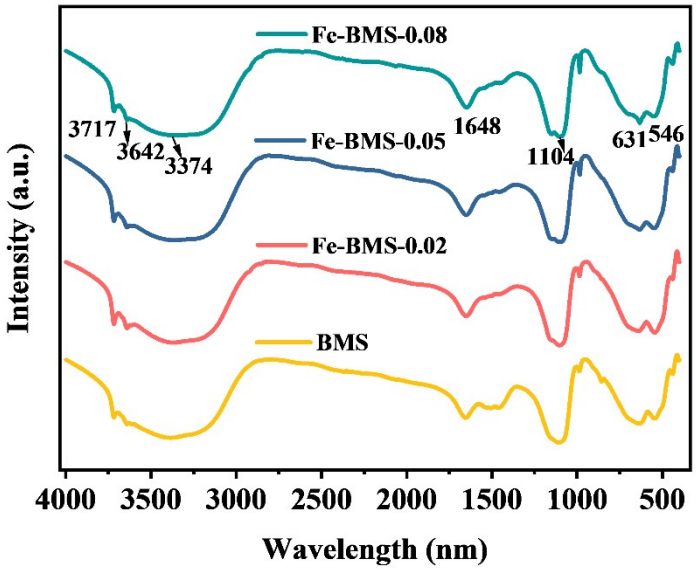

Figure S5. FTIR spectra of BMS and Fe-BMS-x.

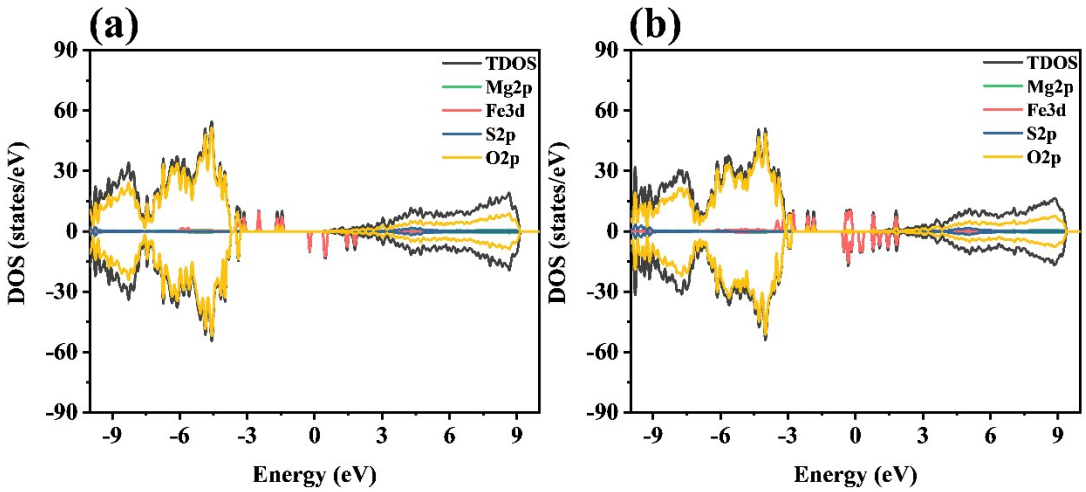

Figure S6. (a) The density of states of Fe-BMS with one Fe atoms replaced, (b) the density of states of Fe-BMS with two Fe atoms replaced.

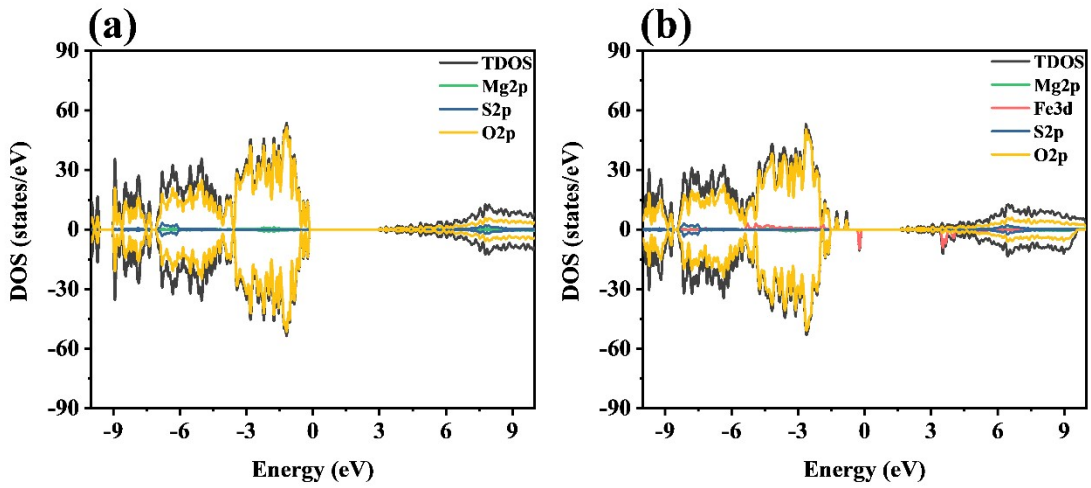

Figure S7. (a) The density of states of BMS with a vacuum layer, (b) the density of states of Fe-BMS with a vacuum layer.

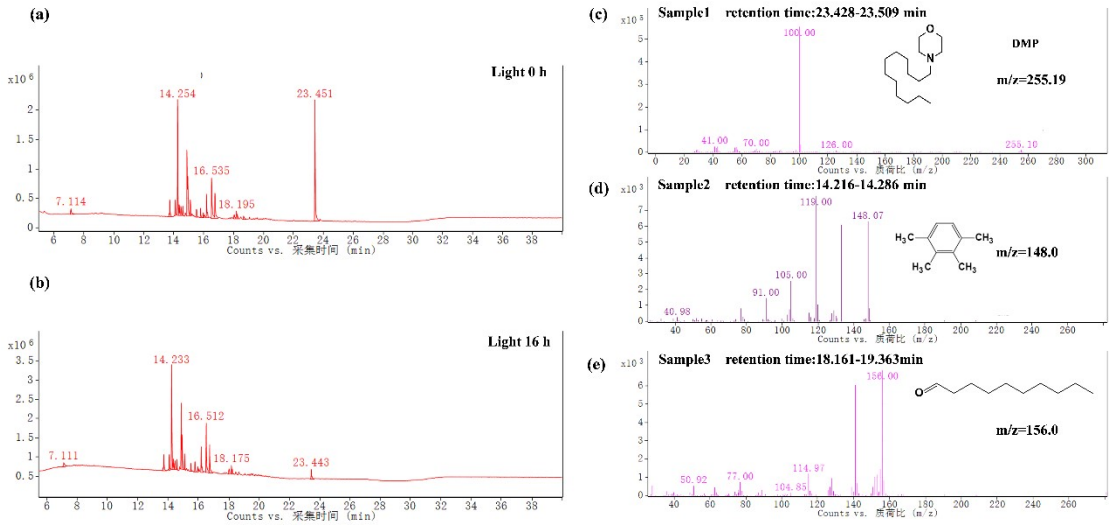

Figure S8. (a-b) Total gas chromatogram of DMP at 0 and 16 hours of photocatalytic degradation by Fe-BMS, (c-e) Mass spectra of main substances appeared in the gas chromatogram.

Table S1. The binding energy and peak area ratio of O1s for BMS and Fe-BMS-x.

O1s (eV)	O1	O2	O3	O1s (%)	O1	O2	O3
BMS	531.73	532.36	533.77		70.52	25.56	3.92
Fe-BMS-0.02	531.68	532.96	533.82		36.58	14.49	48.93
Fe-BMS-0.05	531.63	532.27	533.78		13.44	41.41	45.15
Fe-BMS-0.08	531.67	532.34	533.75		16.21	36.79	47.00

Table S2. TPRL parameters of BMS and Fe-BMS-x.

	τ_1/μs	f_1/%	τ_2/μs	f_2/%	τ_{ave}/μs
BMS	0.27	23.66	3.99	76.34	3.11
Fe-BMS-0.02	0.34	8.80	8.07	91.2	7.39
Fe-BMS-0.05	0.30	13.22	6.20	86.78	5.42
Fe-BMS-0.08	0.27	34.02	2.68	65.98	1.86

Table S3. Comparison of the degradation performance of Methyl orange by photocatalyst Fe-BMS with materials reported in the literature.

Photocatalysts	Dosage	Methyl orange	Adsorption efficiency	Degradation time	Degradation efficiency	Degradation medium	Light source	refs.
MgAl-LDH/g-C_3N_4	100 mg	100 mL (10 mg·L^{-1})	~55%	120 min	94%	liquid phase	300 W Xe-lamp $\lambda > 420$ nm	[1]
$ZnIn_2S_4$/MgAl-LDH-80	10 mg	50 mL (20 mg·L^{-1})	~15%	20 min	100%	liquid phase	300 W Xe-lamp $\lambda > 420$ nm	[2]
1% Fe_2O_3/g-C_3N_4	100 mg	100 mL (10 mg·L^{-1})	~40%	60 min	92%	liquid phase	300 W Xe-lamp $\lambda > 420$ nm	[3]
Fe_2Ce_1O	30 mg	50 mL (100 mg·L^{-1})	0	120 min	85%	liquid phase	300 W Xe-lamp $\lambda > 420$ nm	[4]
Fe-BMS	100 mg	50 mL (20 mg·L^{-1})	~60%	24 h	100%	liquid phase	300 W Xe-lamp simulate sunlight	This work

Table S4. Comparison of the degradation performance of 4-dodecylmorpholine (DMP) by photocatalyst Fe-BMS with materials reported in the literature.

Photocatalysts	Dosage	DMP	Adsorption efficiency	Degradation time	Degradation efficiency	Degradation medium	Light source	refs.
TiO_2-A	120 mg	100 mL (50 mg·L^{-1})	/	300 min	100%	liquid phase	300 W Xe-lamp 280-380 nm	[5]
BMS@TiO_2	100 mg	50 mL (30 mg·L^{-1})	~40%	16 h	92%	air	300 W Xe-lamp 280-380 nm	[6]
CPS (Cu_2O/SnO_2/PDA)	5 mg	5 mL (2 mg·L^{-1})	/	120 min	100%	liquid phase	808 nm near infrared light laser	[7]
WO/gCN-5	100 mg	100 mL (2 mg·L^{-1})	~5%	60 min	73%	liquid phase	300 W Xe-lamp simulate sunlight	[8]
Fe-BMS	100 mg	50 mL (20 mg·L^{-1})	~70%	24 h	96%	liquid phase	300 W Xe-lamp simulate sunlight	This work
Fe-BMS	1000 mg	500 mL (50 mg·L^{-1})	~60%	16 h	54%	gas phase	300 W Xe-lamp simulate sunlight	This work

Table S5. Lattice information after optimization of BMS and Fe-BMS.

Sample	a(Å)	b(Å)	c(Å)	alpha(°)	beta(°)	gamma(°)	Number of atoms	Mg	H	S	O	Fe
BMS-unoptimized	10.0141	12.687	14.5846	90	103.8965	90		24	96	4	84	/

BMS	10.01165	12.69041	14.53398	90	104.0619	90	24	96	4	84	/
Fe-BMS	10.00262	12.71121	14.54004	90	104.1115	90	23	96	4	84	1

Table S6. The variance of bond lengths and bond angles of Fe-BMS and Fe-BMS with a vacuum layer.

Sample	Parameter	Average value	Variance
Fe-BMS	Bond length (Å)	2.16798	0.00711
	Bond angle (°)	89.99272	99.31711
Fe-BMS with a vacuum layer	Bond length (Å)	2.15957	0.00335
	Bond angle (°)	90.06590	91.19651

Reference

1 T.R. Hao, H.L. Xu, S.P. Sun, H. Yan, Q.Q. Qin, B. Song, M.L. Li, G. Shao, B.B. Fan, H.L. Wang, H.X. Lu, *Ceram. Int.*, 2024, **50**,10724-10734.

2 Q. Gao, L.C. Ye, W. Liu, J.X. Li, Y.C. Cui, N.C. Xu, M.J. Zhang, *Environ. Sci.:Water Res. Technol.*, 2024, **10**, 2589-2596.

3 L. Wei, X.Q. Zhang, J. Wang, J. Yang, X.D. Yang, *Inorg. Chem. Commun.*, 2024, **159**, 11890.

4 L. Li, C.Q. Wu, D.X. Sun, N. Zhang, T. Huang, Y. Wang, *J. Cleaner Prod.*, 2024, **483**, 144293.

5 L. Ma, M. Lu, K.X. Li, S.Y. Zhang, H. N. Liu, Y.F. Huang, Z. Xing, Z.J. Wu, X.S. Ye, *Chem. Eng. J.*, 2023, **472**, 144782.

6 Z.M. Song, H.F. Zhang, L. Ma, M. Lu, C.Y. Wu, Q.Q. Liu, X.F. Yu, H.N. Liu, X.S. Ye, Z. Ma, Z.J. Wu, *Sci. Rep.*, 2024, **14**, 9315.

7 P.S. Guo, D.M. Yu, C.T. Zhao, J.P. Wang, J. Cheng, W.X. Fan, T.T. Ma, T. Gao, J.H. Li, *J. Environ. Chem. Eng.*, 2024, **12**, 114682.

8 L.X. Zheng, Y.L. Wei, C.Y. Wang, H.N. Liu, L.Y. Li, M.L. Huang, Y.F. Huang, L.Q. Fan, J.H. Wu, *Ceram. Int.*, 2024, **50**, 38860-38870.